

Synthesis, Chain Rigidity, and Luminescent Properties of Poly[(1,3-phenyleneethynylene)-*alt*-tris(2,5-dialkoxy-1,4-phenyleneethynylene)]s

Qinghui Chu and Yi Pang*

Department of Chemistry & Center for High Performance Polymers and Composites, Clark Atlanta University, Atlanta, Georgia 30314

Liming Ding and Frank E. Karasz

Department of Polymer Science and Engineering, University of Massachusetts, Amherst, Massachusetts 01003

Received June 10, 2002; Revised Manuscript Received August 1, 2002

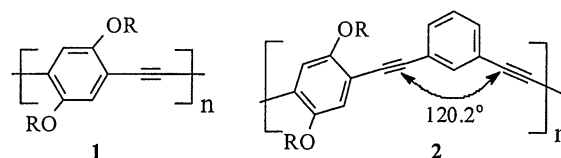
ABSTRACT: Soluble poly[(1,3-phenyleneethynylene)-*alt*-tris(2,5-dialkoxy-1,4-phenyleneethynylene)] derivatives (**5**) have been synthesized by using the Heck-type coupling reaction. Even with a significant increase in the *p*-phenyleneethynylene content, the copolymers exhibit a random-coil conformation in THF solution, with a Mark–Houwink exponent determined to be $\alpha \approx 0.78$. As a result of the extended conjugation length of the chromophore, the absorption and emission λ_{max} values of **5** are notably red-shifted (by about 30–40 nm) from that of poly[(1,3-phenyleneethynylene)-*alt*-(2,5-dialkoxy-1,4-phenyleneethynylene)] derivatives (**2**). The fluorescence quantum efficiency of **5** is estimated to be $\phi_{\text{f}} \approx 0.50$, slightly higher than that of **2** ($\phi_{\text{f}} \approx 0.44$). The fluorescence of **5** in the solid state is strong, indicating its potential for various device applications. LEDs based on **5** emitted green-yellow EL with an external quantum efficiency of 0.013%.

Introduction

The use of fluorescent π -conjugated polymers in emerging technologies, such as LED displays,¹ sensors,² and lasers,³ is rapidly expanding since the first demonstration of a LED device using these polymers.⁴ As an important example in the field, poly(*p*-phenyleneethynylene) (PPE) derivatives⁵ have also exhibited many attractive properties. Incorporation of a *m*-phenylene linkage along the PPE backbone⁶ effectively interrupts the π -conjugation, thereby leading to chromophores with defined conjugation length. Introduction of a bent angle along the polymer backbone at the *m*-phenylene group clearly modifies the chain stiffness, thus leading to the simultaneous improvement⁶ in both solubility and luminescence efficiency. Although poly(*m*-phenyleneethynylene)⁷ of high molecular weights is insoluble, the alternating copolymer **2** with both *p*- and *m*-phenylene units exhibits good solubility in common organic solvents.

As a result of the linear bond geometry of acetylene and *p*-phenylene linkages, the polymer backbone of **1** is expected to exhibit a rigid-rod conformation, which is of fundamental and theoretical interest. The Mark–Houwink exponent⁸ of **1** has been reported to be $\alpha \approx 1.92$, consisting with its high chain stiffness. A light-scattering study⁹ shows that the polymer conformation is nearly rodlike for relative low M_w (<50 000) but appears to be coillike in solution for the high molecular weights. Introduction of a bent angle along the polymer backbone at the *m*-phenylene, however, drastically lowers the Mark–Houwink α exponent to about 0.65 for polymer **2**.⁶ A fundamental question remains whether a smaller percentage (i.e., < 50%) of *m*-phenylene units will be sufficient to improve the solubility and processability of PPEs. To further evaluate the impact of *m*-phenylene to the chain rigidity of PPEs, we have synthesized polymer **5**, in which the content of *m*-phenylene is decreased to 25%. The higher content of

p-phenylene in **5** will also tune the emission color (red shift relative to **2**), thereby expanding the application scope of these *m*-phenylene-based polymers. The regular location of the *m*-phenyleneethynylene unit along the backbone of **5**, following three consecutive *p*-phenyleneethynylene units, leads to a polymer with a uniformly defined chromophore structure. In this contribution, we wish to report the synthesis, chain rigidity, and optical properties of **5**.



Results and Discussion

Polymer Synthesis and Characterization. The desired monomer, 1,3-bis[(2,5-dibutoxy-4-ethynylphenyl)ethynyl]benzene derivative **4** (Scheme 1), was conveniently synthesized by reacting 2,5-dibutoxy-1-trimethylsilylethynyl-4-ethynylbenzene (**3**) with 1,3-diiodobenzene derivatives in the presence of palladium catalyst¹⁰ (Sonogashira–Hagihara coupling).¹¹ Polymerization of **4** with 2,5-dibutoxy-1,4-diiodobenzene gave the desired polymer **5** as a yellow solid after precipitation from methanol. Infrared spectra of polymer films detected no absorbance at $\sim 3290 \text{ cm}^{-1}$ (acetylenic C–H stretch), which is moderately strong in the monomer **4**. Complete polymerization was further confirmed by the ¹H NMR spectra, which showed no acetylenic resonance signals at $\sim 3.35 \text{ ppm}$ (Figure 1). The resonance signals at about 4.04 and 4.34 ppm (in a ratio of 6:1) in the ¹H NMR spectrum of **5b** can be attributed to $-\text{OCH}_2-$ protons from the alkoxy side chain on the *p*-phenylene and *m*-phenylene, respectively. The presence of only one Ar–CH₃ resonance signal at $\sim 2.25 \text{ ppm}$ supports the

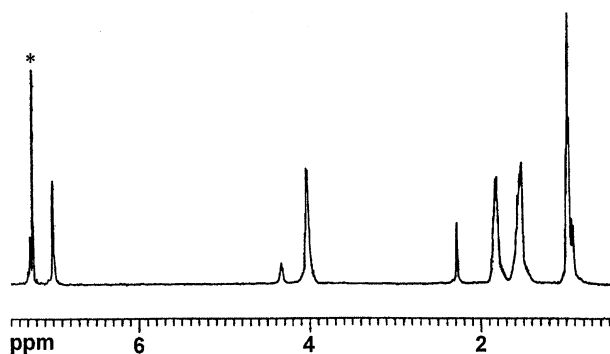
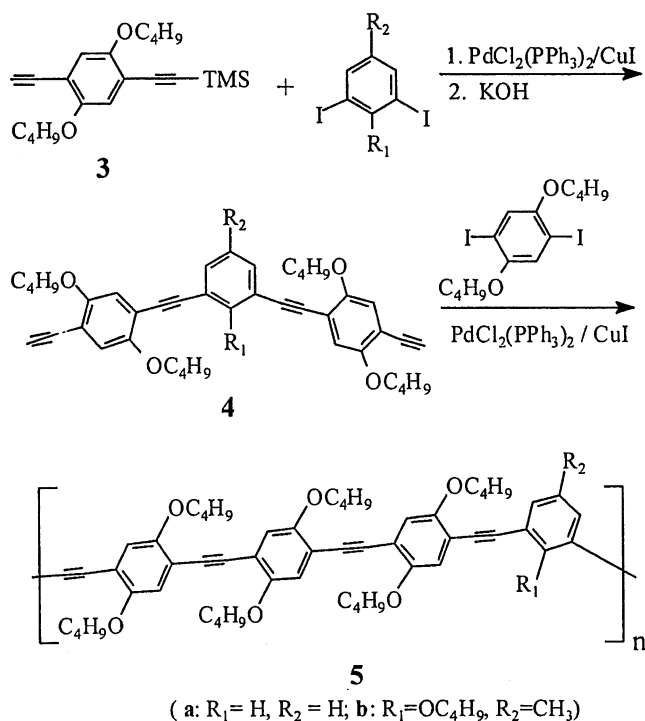


Figure 1. ^1H NMR spectrum of **5b** in CDCl_3 . The starred resonance signal at 7.25 ppm is attributed to CHCl_3 .

Scheme 1. Polymer Synthesis

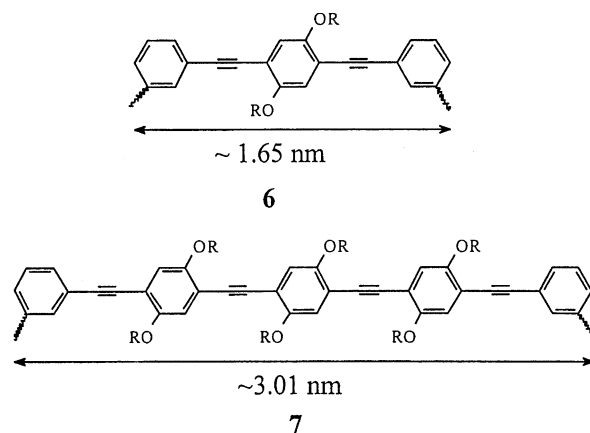


structural regularity along the polymer backbone. Although bearing only short *n*-butyl side chains, polymer **5** was quite soluble in the common organic solvents such as toluene, chloroform, and THF. Uniform thin films could be readily cast from their solutions.

Molecular Weight and Chain Stiffness. The molecular weights of **5**, which are listed in Table 1, were determined in THF by using size exclusion chromatography (SEC) equipped with on-line refractive index (RI), light scattering (LS), and viscometer detectors (Figure 2). The combination of high molecular weight, low polydispersity (PDI), and monomodal distribution, in addition to the high polymerization yield ($\sim 80\%$), suggested that the polymerization proceeded smoothly as expected. The number-average degree of polymerization (DP) was estimated to be $n \approx 13$ for **5a** and $n \approx 27$ for **5b** by using the respective M_n and molecular weight of the repeating unit (833 and 919 for **5a** and **5b**, respectively).

By using the on-line viscometer detector, the Mark–Houwink α exponent for polymer **5** was estimated to be ~ 0.78 in THF solvent at room temperature, which is only slightly higher than $\alpha \approx 0.65$ for **2**. The instrument was calibrated by using a broad polystyrene standard,

which gave an α value of 0.714 (in agreement with the literature value).¹² An overlay of the Mark–Houwink plot is shown in Figure 3, displaying the difference between polymers **2** and **5**. For each polymer, a fairly good linearity was observed between $\log[\eta]$ and $\log(M_w)$ within the molecular weight range of the sample, which supports the proposed linear polymer structure and indicates the absence of chain branching. The polymer backbone of **5** can be simply viewed as a series of the rigid-rod components **7** joined together via sharing the common *m*-phenylene linkages. Although the rigid-rod length is significantly increased from ~ 1.65 nm (for **2**) to ~ 3.01 nm (for **5**),¹³ the α value of the polymer is only slightly increased. In summary, the observed Mark–Houwink exponent ($\alpha \approx 0.78$) shows that the polymer **5** adopts a random-coil conformation¹⁴ in THF solution.



Photoabsorption and Photoluminescence (PL).

The UV–vis absorption of **5** in dilute THF (Figure 4) showed a major band at ~ 397 nm (low-energy band) and a minor band at about 311 nm (high-energy band). In comparison with **2**, the absorption λ_{max} of **5** is noticeably red-shifted from about 376 nm for **2** to ~ 397 nm for **5**. As a result of the effective π -conjugation interruption at the *m*-phenylene, the effective chromophore for polymers **2** and **5** may be represented by the molecular fragments **6** and **7**, respectively. The bathochromic shift observed from **2** to **5**, therefore, is due to the extended conjugation length in the latter. It is also noted that the high-energy absorption band at ~ 311 nm remained similar for both **2** and **5**. The relative intensity of the high-energy absorption band, however, decreases with the increased conjugation length. The trend is also consistent with the results observed from **2** and its *p*-phenylene isomer poly[(2,5-dialkoxy-1,4-phenylenevinylene)-*alt*-(1,4-phenylenevinylene)].⁶

The emission profile of **5** is very similar to that of **2**, although the emission λ_{max} of the former is significantly red-shifted from that of the latter (447 nm vs 405 nm). It is also noticed that the peak width of **5** is essentially the same as that of **2**, with the peak width at half-height of ~ 34 nm. The narrow emission characteristics of **5** is in agreement with the assumption that the chromophore in the polymer is uniformly defined. The fluorescence quantum efficiency (ϕ_f) of **5** is higher than that of **2**, which could be partially attributed to the higher chain rigidity of the former. The longer conjugation length of **5** (relative to **2**) could be another reason for its high ϕ_f value.

The emission spectrum of **5** at 25 °C exhibited one major peak at about 447 nm and a shoulder at about

Table 1. Molecular Weights and Spectroscopic Data of PPEs

polymers	M_w	PDI	DP	α^a	UV-vis λ_{\max} (nm) ^b		fluorescence λ_{\max} (nm)		ϕ_f^c
					THF	film	THF	film	
5a	19 700	1.8	13	0.779	311, 397	325, 414, 446	447 , 469 (sh)	487 , 513	0.49
5b	55 100	2.2	27	0.776	318, 410	327, 417, 450	449 , 468 (sh)	491 , 520	0.50
2 (R = <i>n</i> -hexyl)	176 900	1.6	276	0.650	312, 376	315, 383	405 , 427 (sh)	471 , 494 (sh)	0.44

^a Mark-Houwink exponent were measured in THF at room temperature. ^b The bold number indicates the most intense peak. ^c The ϕ_f values were averaged over three independent measurements.

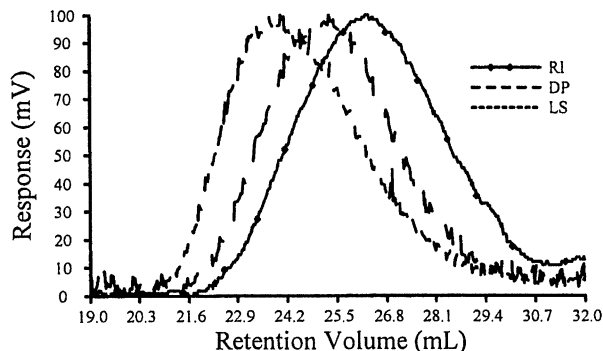


Figure 2. SEC chromatogram of **5a**. Curves RI, DP, and LS are respective responses from refractive index, viscosity, and light-scattering detectors.

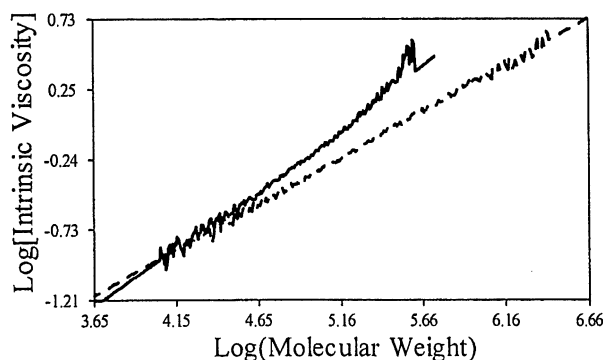


Figure 3. Overlay Mark-Houwink plot for **5b** (dotted line) and **2** (solid line, R = *n*-hexyl). The small peak in the plot of **5b** at $\log(M_w) \approx 5.6$ is due to the instrument noise from low concentration at the high M_w end.

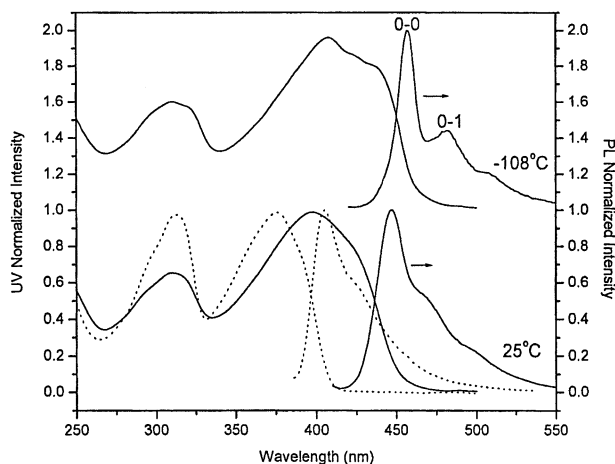


Figure 4. Normalized UV-vis and PL spectra of polymers **5b** (solid line) and **2** (dotted line) in THF.

469 nm (Figure 4), indicating the existence of vibronic structure. As the temperature was lowered to -108 °C, several emission bands were observed with λ_{\max} values at 457, 482, and ~ 510 nm (corresponding to 21 882, 20 747, and 19 608 cm^{-1} , respectively). The vibrational

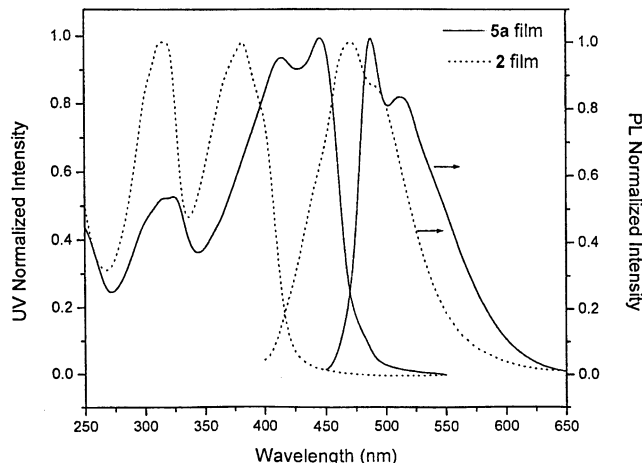


Figure 5. Normalized UV-vis and PL spectra of films **5a** (solid line) and **2** (dotted line).

energy levels in the ground state of **5** (shown from the emission spectrum) appeared to be about equally spaced with a wavenumber separation of ~ 1135 cm^{-1} , which is expected from a harmonic oscillator model.¹⁵ The UV-vis absorption spectrum of **5** was also partially resolved at -108 °C, showing an obvious shoulder at ~ 440 nm ($22\,727$ cm^{-1}). This absorption band ($\lambda_{\max} \approx 440$ nm) was separated from the emission band of the highest energy ($\lambda_{\max} = 457$ nm) by ~ 845 cm^{-1} , which is smaller than the required energy gap of 1135 cm^{-1} for a lower energy level in a harmonic oscillator model. The emission bands at 457, 482, and ~ 510 nm, therefore, are attributed to 0-0, 0-1, and 0-2 transitions, respectively.

To examine the optical properties in the solid state, polymer films of **2** and **5** were prepared by spin-casting their solutions onto quartz substrates. The absorption λ_{\max} of films **5a** and **5b** were red-shifted by about 40 nm relative to their respective solution spectra (Table 1), while the film **2** was red-shifted by only ~ 7 nm. The larger bathochromic shift observed from **5** in the absorption spectra is in agreement with the anticipated stronger interaction between chromophores of larger dimension (longer rigid rod) in the solid state. The emission spectra of both films **2**¹⁶ and **5** were significantly red-shifted from their respective solution spectra (~ 66 nm for the former and ~ 40 nm for the latter). The interesting pattern that a significant spectroscopic red shift from the solution to film states is observed from both the absorption and emission of **5**, but only from the emission of **2**, indicates that a strong polymer chain-chain interaction may start to occur even in the ground state of film **5**. It is also noticed that the absorption and emission spectra of **5** in the solid state become slightly more structured (Figure 5) in comparison with their corresponding solution spectra at room temperature. The high-energy emission peak of **5a** ($\lambda_{\max} = 487$ nm) falls at the edge of its absorption profile,

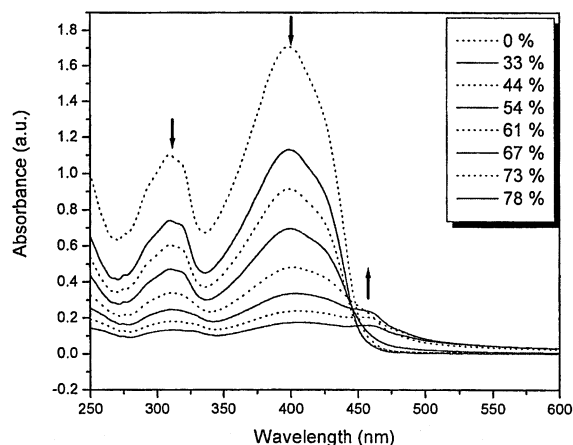


Figure 6. UV-vis absorption spectra of **5a** in THF/methanol mixtures. The solvent composition is marked by the volume percentage of methanol. Arrows indicate the decline or growth of bands with increasing methanol concentration. The spectra are plotted alternately with solid and dotted line for clarity.

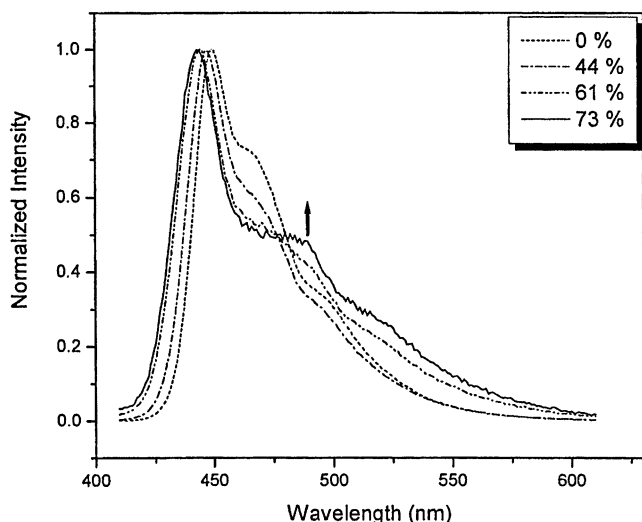


Figure 7. Emission spectra of **5a** in solvent/nonsolvent (THF/methanol) mixtures. The arrow indicates the growth of band with increasing methanol concentration. The solvent composition is marked by the volume percentage of methanol.

suggesting that the emission band at $\lambda_{\text{max}} = 487$ nm might originate from a 0-0 transition.

Molecular Aggregation. UV-vis spectra of **5** in a solvent/nonsolvent (THF/methanol) mixture were acquired to detect the possible formation of molecular aggregate in solution, which has been observed from a limited examples of poly(*p*-phenyleneethynylene) derivatives.¹⁷ As shown in Figure 6, a new absorption band at ~ 460 nm was gradually developed when the methanol concentration was higher than $\sim 61\%$. This new absorption band at ~ 460 nm was similar to that observed from its film, suggesting the formation of molecular aggregates in solution. Fluorescence spectra of **5** in various solvent/nonsolvent compositions showed a new band at ~ 488 nm (marked by an arrow in Figure 7), whose emission intensity gradually increased with the methanol concentration. It should be noted that the new emission band occurred at the same position as the polymer film (emission $\lambda_{\text{max}} = 487$ nm), further supporting the assumption of aggregate formation in the solution of **5**. UV-vis spectra of **2** did not detect any molecular aggregate in the same solvent/nonsolvent system. The trend of the aggregate formation appeared

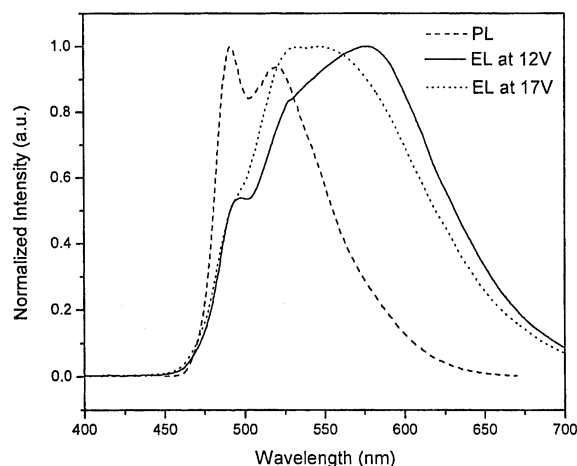


Figure 8. Electroluminescence spectra for a ITO/PEDOT/**5b**/Ca/Al LED at 12 and 17 V. The PL spectrum of film **5b** is shown for comparison.

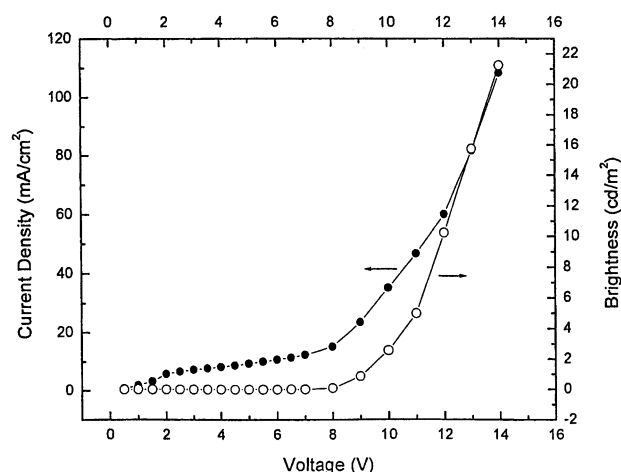


Figure 9. Current density (●)-voltage-brightness (○) relationship for device ITO/PEDOT/**5b**/Ca/Al.

to be consistent with the polymer chain rigidity, as the more rigid polymer **5** exhibited a higher tendency for molecular aggregate than **2**. The higher tendency for **5** to form the molecular aggregate also agrees with its stronger polymer chain-chain interaction.

EL Properties. The high luminescence of the polymer films of **5** indicated potential applications in various devices. A double-layer LED with the ITO/PEDOT/polymer/Ca/Al configuration utilizing polymer **5b** as the emissive layer was fabricated. The device emits green-yellow light as shown in Figure 8. The EL spectra show an obvious voltage dependence: at 12 and 17 V, the EL peak wavelengths are 577 and 547 nm, respectively. Thus, with an increase of the applied voltage, the EL spectra show a remarkable blue shift of 30 nm. This change in EL is due to Joule heating of the LED at higher current density, which results in a thermochromic effect.^{18,19} The phenomenon can also result from a band-gap distribution in the polymer.²⁰ At the higher applied voltage, emission from the higher band-gap segments contributes more to the spectrum. Compared with the solid-state PL spectrum of **5b**, the EL spectra show obvious red shifts and a substantial spectral broadening. This results from LED interface effects²¹ and structural defects in the polymer.²²⁻²⁴ The tailing in the long wavelength region can be due to defects in the emissive polymer layer which act as new recombination centers in which excitons radiatively decay,

yielding an emission different from that given by excitons decaying on the pristine polymer main chain. The LED using **5b** has a turn-on voltage of 8 V and has an external quantum efficiency of 0.013%.

It should be noted that the 0–0 emission band at ~490 nm, which is the most intense photoluminescent emission, becomes the minor peak in the EL spectrum. The 0–1 emission band at ~520 nm, which is well-resolved in the PL spectrum, is also observable in the EL spectrum. While emission from the higher vibronic transitions remains a possibility to account for the red-shifted EL emission, the possible presence of a second optically active species and the formation of an exciplex may also contribute to the spectral mismatch between the PL and EL profiles.

Conclusion

Poly[(1,3-phenyleneethynylene)-*alt*-tris(2,5-dialkoxy-1,4-phenyleneethynylene)] derivatives (**5**) have been synthesized and characterized. Molecular modeling studies show that the length of the linear rigid-rod PPE fragment in **5** is about 3.01 nm, which is nearly twice as long as 1.65 nm for poly[(1,3-phenyleneethynylene)-*alt*-(1,4-phenyleneethynylene)] derivatives (**2**). Despite the significant increase in the length of the rigid-rod component, polymer **5** still exhibits a random-coil conformation in THF solution, with a Mark–Houwink exponent $\alpha \approx 0.78$. Good solubility of **5** in common organic solvents suggests that incorporation of even smaller fraction (<25%) of *m*-phenylene unit may be sufficient to provide the desired solubility. The increased length of the rigid-rod PPE fragment in **5** also extends the conjugation length of the chromophore, thereby tuning the emission color of the *m*-phenylene-based polymers. The films of polymer **5** give intense PL, suggesting potential applications in various devices. LEDs of **5** emit green-yellow color with an external quantum efficiency of 0.013%. Future study will focus on further improving the luminescence quantum efficiency and emission characteristics of the materials. The increased chain rigidity of **5** also aids the aggregate formation, which will be further investigated in the future.

Experimental Section

Materials and Measurements. 2-Butoxy-1,3-diiodo-5-methylbenzenes,²⁵ 2,5-diiodo-1,4-dibutoxybenzene,²⁶ and 1,4-dibutoxy-2,5-diethynylbenzene²⁷ were prepared according to literature procedures. NMR spectra were collected on a 400 MHz Bruker ARX-400 spectrometer. Infrared spectra were recorded on a Nicolet Impact 400 FT-IR spectrometer. UV–vis spectra were acquired on a Hewlett-Packard 8453 diode array spectrophotometer. Fluorescence spectra were obtained on a PTI steady-state fluorometer. Size exclusion chromatography (SEC) was carried out on a Viscotek SEC assembly consisting of a model P1000 pump, a model T60 dual detector, a model LR40 laser refractometer, and three mixed bed columns (10 μ m). Polymer concentrations for SEC experiments were prepared in a concentration of about 3 mg/mL. The SEC system was calibrated by using narrow and broad polystyrene standards prior to use. The polystyrene standards were purchased from American Polymer Standards Corp.

2,5-Dibutoxy-1-ethynyl-4-(trimethylsilylethynyl)benzene (3). To a flame-dried and argon-purged flask were added THF (200 mL) and 1,4-dibutoxy-2,5-diethynylbenzene (3.24 g, 12 mmol). The mixture was cooled to -78°C , and *n*-BuLi (4.8 mL, 2.5 M in hexane) was added via a syringe over 1 h. After stirring at -78°C for 2 h, trimethylsilyl chloride (2.5 mL, 20 mmol) was added to the reaction mixture. The reaction mixture

was gradually warmed to room temperature and stirred overnight. The resulting solution was concentrated under vacuum, and the residue was dissolved in hexane. The precipitated salts were removed via filtration, and the solvents were evaporated on a rotatory evaporator. The desired product (3.33 g, 81%) was obtained as yellowish crystals (mp = $73\text{--}74^\circ\text{C}$) after purification on a silica gel column using a mixture of hexane and ethyl acetate (1:40) as eluent. ^1H NMR (CDCl_3 , 400 MHz): δ 0.24 (s, 9H, $-\text{Si}(\text{CH}_3)_3$), 0.97 (t, $J = 6.8$ Hz, 6H, $-\text{CH}_3$), 1.50 (m, 4H, $-\text{CH}_2-$), 1.75 (m, 4H, $-\text{CH}_2-$), 3.30 (s, 1H, $-\text{C}\equiv\text{CH}$), 3.95 (t, $J = 6.4$ Hz, 4H, $-\text{OCH}_2-$), 6.91 (s, 2H, Ar–H). ^{13}C NMR (CDCl_3 , 100 MHz): δ -0.39 , 13.54, 18.94, 31.08, 68.98, 79.60, 82.08, 99.82, 100.82, 112.67, 114.19, 116.91, 117.55, 153.76. Anal. Calcd for $\text{C}_{21}\text{H}_{30}\text{O}_2\text{Si}$: C, 73.63; H, 8.83. Found: C, 73.38; H 8.78.

1,3-Bis(4-ethynyl-2,5-dibutoxyphenyl-1-ethynyl)benzene (4a). 1,3-Diiodobenzene (0.3299 g, 1 mmol) and **3** (0.6491 g, 2 mmol) were dissolved in a mixture of solvents consisting of toluene (20 mL) and triethylamine (2 mL) in a 50 mL round-bottomed flask. After replacing the air with argon in the flask, $\text{PdCl}_2(\text{PPh}_3)_2$ (8 mg, 1 mol %) and CuI (4 mg, 2 mol %) were added. The reaction mixture was then stirred overnight at room temperature under positive argon atmosphere. The resulting solution was passed through a thin layer of Celite to remove salts and catalysts, and the solvents were evaporated. Purification on a silica gel column (eluent: ethyl acetate/hexanes = 1:10) gave 1,3-bis(4-trimethylsilylethynyl-2,5-dibutoxyphenyl-1-ethynyl)benzene, which was further treated with KOH (0.03 g) in a solvent mixture of methanol and THF (1:1) at room temperature. The desired product **4a** was isolated on a silica gel column (0.37 g, 80%) and had the following spectral properties. ^1H NMR (CDCl_3 , 400 MHz, δ): 0.99 (t, $J = 6.8$ Hz, 12H, $-\text{CH}_3$), 1.58 (m, 8H, $-\text{CH}_2-$), 1.85 (m, 8H, $-\text{CH}_2-$), 3.36 (s, 2H, $-\text{C}\equiv\text{CH}$), 4.04 (t, $J = 6.4$ Hz, 8H, $-\text{OCH}_2-$), 6.98 (s, 4H, Ar–H), 7.38 (t, $J = 8.0$ Hz, 1H, Ar'–H), 7.51 (d, $J = 8.0$ Hz, 2H, Ar'–H), 7.71 (s, 1H, Ar'–H). ^{13}C NMR (CDCl_3 , 100 MHz, δ): 13.58, 18.90, 30.98, 69.12, 79.69, 82.09, 86.07, 93.72, 112.59, 114.15, 116.72, 117.62, 123.48, 128.18, 131.03, 134.21, 153.27, 153.90. IR (film): 3290 (m), 2959 (s), 2926 (s), 2870 (m), 2210 (w), 2106 (w), 1497 (s), 1385 (m), 1215 (s), 1026 (m), 862 (m). Anal. Calcd for $\text{C}_{42}\text{H}_{46}\text{O}_4$: C, 82.05; H, 7.54. Found: C, 82.18; H, 7.62.

2-Butoxy-1,3-bis(4-ethynyl-2,5-dibutoxyphenyl-1-ethynyl)-5-methylbenzene (4b). The synthesis of **4b** was similar to that described for **4a**, using 2-butoxy-1,3-diiodo-5-methylbenzene instead of 1,3-diiodobenzene. The desired product was obtained as a yellow solid (mp = $89\text{--}90^\circ\text{C}$) and had the following spectral properties. ^1H NMR (CDCl_3 , 400 MHz, δ): 1.00 (s, 15H, $-\text{CH}_3$), 1.52 (m, 10H, $-\text{CH}_2-$), 1.82 (m, 10H, $-\text{CH}_2-$), 2.31 (s, 3H, Ar'–CH₃), 3.35 (s, 2H, $-\text{C}\equiv\text{CH}$), 4.02 (t, $J = 6.4$ Hz, 8H, $-\text{OCH}_2-$), 4.36 (t, $J = 6.4$ Hz, 2H, $-\text{OCH}_2-$), 6.99 (s, 4H, Ar–H), 7.29 (s, 2H, Ar'–H). ^{13}C NMR (CDCl_3 , 100 MHz, δ): 13.56, 18.90, 20.10, 31.08, 32.33, 69.06, 73.90, 79.75, 82.01, 89.46, 90.98, 112.37, 114.58, 116.78, 117.20, 117.52, 132.35, 133.99, 153.13, 153.85, 158.62. IR (film): 3290 (m), 2957 (m), 2870 (m), 2201 (w), 2098 (w), 1500 (s), 1390 (m), 1217 (s), 1030 (m), 854 (m). Anal. Calcd for $\text{C}_{47}\text{H}_{56}\text{O}_5$: C, 80.53; H, 8.05. Found: C, 80.48; H, 8.08.

Synthesis of Polymer 5a. 2,5-Diiodo-1,4-bis(butoxy)benzene (0.4741 g, 1 mmol), **4a** (0.6148 g, 1 mmol), and triethylamine (7 mmol) were dissolved in dry toluene (20 mL). The solution was deoxygenated by three times repeating the cycle of freezing and thawing under vacuum, followed by filling with an argon atmosphere. After adding catalysts $\text{PdCl}_2(\text{PPh}_3)_2$ (1 mol %) and CuI (2 mol %) under the argon atmosphere, the reaction mixture was stirred at room temperature for 24 h. The resulting fluorescent solution was filtered through a thin layer of Celite to remove salts and catalysts. After precipitation from methanol, polymer **4a** (0.65 g, 78%) was obtained as a yellow powder after drying in a vacuum oven at 40°C for 24 h. ^1H NMR (CDCl_3 , 400 MHz, δ): 1.01 (s, 18H, $-\text{CH}_3$), 1.54 (m, 12H, $-\text{CH}_2-$), 1.86 (m, 12H, $-\text{CH}_2-$), 4.01 (s, 12H, $-\text{OCH}_2-$), 7.01 (s, 6H, Ar–H), 7.33 (t, $J = 7.7$ Hz, 1H, Ar–H), 7.50 (d, $J = 7.7$ Hz, 2H, Ar–H), 7.69 (s, 1H, Ar–H). IR (film): 2967 (m), 2932 (m), 2870 (m), 2208 (w), 1506 (m), 1423

(m), 1213 (s), 1025 (m). Anal. Calcd for $C_{56}H_{64}O_6$: C, 80.73; H, 7.74. Found: C, 79.48; H, 7.28.

Polymer 5b (0.74 g, 80%) was obtained as a yellow powder and had the following spectral properties. 1H NMR ($CDCl_3$, 400 MHz, δ): 0.99 (m, 21H, $-CH_3$), 1.52 (m, 14H, $-CH_2-$), 1.83 (m, 14H, $-CH_2-$), 2.29 (s, 3H, Ar- CH_3), 4.04 (s, 12H, $-OCH_2-$), 4.34 (s, 2H, $-OCH_2-$), 7.01 (s, 6H, Ar-H), 7.29 (s, 2H, Ar'-H). IR (film): 2957 (m), 2930 (m), 2870 (m), 2206 (w), 1510 (w), 1425 (s), 1211 (s), 1026 (m), 860 (m). Anal. Calcd for $C_{61}H_{74}O_7$: C, 79.70; H, 8.11. Found: C, 78.81; H, 8.08.

LED Device Fabrication and Measurement. PEDOT/PSS (Bayer Co.) was spin-cast onto ITO glass (OFC Co.) used as an anode. The polymer solutions (20 mg/mL in chloroform) were filtered through 0.2 μm Millex-FGS Filters (Millipore Co.) and were spin-cast onto dried PEDOT/ITO substrates under a nitrogen atmosphere. The polymer films were typically 75 nm thick. Calcium electrodes of 400 nm thickness were evaporated onto the polymer films at about 10^{-7} Torr, followed by a protective coating of aluminum. The devices were characterized using a system constructed in our laboratory described elsewhere.²⁸

Acknowledgment. Support of this work has been provided by AFOSR (Grant F49620-00-1-0090). Partial support from NASA through High Performance Polymers and Composites Center is also acknowledged. We also thank a referee for helpful suggestions.

References and Notes

- (1) Kraft, A.; Grimsdale, A. C.; Holmes, A. B. *Angew. Chem., Int. Ed.* **1998**, *37*, 402–428.
- (2) McQuade, D. T.; Pullen, A. E.; Swager, T. M. *Chem. Rev.* **2000**, *100*, 2537–2574.
- (3) McGehee, M. D.; Heeger, A. J. *Adv. Mater.* **2000**, *12*, 1655–1668.
- (4) Burroughes, J. H.; Bradley, D. D. C.; Brown, A. R.; Marks, R. N.; Mackay, K.; Friend, R. H.; Burn, P. L.; Holmes, A. B. *Nature (London)* **1990**, *347*, 539–541.
- (5) Bunz, U. H. F. *Chem. Rev.* **2000**, *100*, 1605–1644.
- (6) Pang, Y.; Li, J.; Hu, B.; Karasz, F. E. *Macromolecules* **1998**, *31*, 6730–6732.
- (7) Trumbo, D. L.; Marvel, C. S. *J. Polym. Sci., Polym. Chem.* **1986**, *24*, 2311–2326.
- (8) Moroni, M.; Moigne, J. L.; Luzzati, S. *Macromolecules* **1994**, *27*, 562–571.
- (9) Cotts, P. M.; Swager, T. M.; Zhou, Q. *Macromolecules* **1996**, *29*, 7323–7328.
- (10) Sanechika, K.; Yamamoto, T.; Yamamoto, A. *Bull. Chem. Soc. Jpn.* **1984**, *57*, 752–755.
- (11) Sonogashira, K. *J. Organomet. Chem.* **2002**, *653*, 46–49.
- (12) Kurata, M.; Tsunashima, Y. In *Polymer Handbook*, 3rd ed.; Brandrup, J., Immergut, E. H., Eds.; John Wiley and Sons: New York, 1989; p VII/1&16.
- (13) The molecular geometry of the PPE oligomers **6** and **7** was optimized, and their linear dimensions were measured by using HyperChem 6.0 software with AM1 Semi-Empirical setting.
- (14) Sperling, L. H. *Introduction to Physical Polymer Science*, 2nd ed.; John Wiley and Sons: New York, 1992; pp 104, 297.
- (15) Turro, N. J. *Modern Molecular Photochemistry*; University Science: Mill Valley, CA, 1991; Chapter 4.
- (16) The PL spectrum of film **2** is acquired on a quartz substrate, which is different from that⁶ on the ITO substrate reported previously.
- (17) Halkyard, C. E.; Rampey, M. E.; Kloppenburg, L.; Studer-Martinez, S. L.; Bunz, U. H. F. *Macromolecules* **1998**, *31*, 8655–8659.
- (18) Braun, D.; Heeger, A. J. *Appl. Phys. Lett.* **1991**, *58*, 1982–1984.
- (19) Braun, D.; Moses, D.; Zhang, C.; Heeger, A. J. *Appl. Phys. Lett.* **1992**, *61*, 3092–3094.
- (20) Bolognesi, A.; Bajo, G.; Paloheimo, J.; Östergård, T.; Stubb, H. *Adv. Mater.* **1997**, *9*, 121–124.
- (21) Meng, H.; Yu, W.; Huang, W. *Macromolecules* **1999**, *32*, 8841–8847.
- (22) Tao, X.; Zhang, Y.; Wada, T.; Sasabe, H.; Suzuki, H.; Watanabe, T.; Miyata, S. *Adv. Mater.* **1998**, *10*, 226–230.
- (23) Montali, A.; Smith, P.; Weder, C. *Synth. Met.* **1998**, *97*, 123–126.
- (24) Ng, S.; Lu, H.; Chan, H.; Fujii, A.; Laga, T.; Yoshino, K. *Adv. Mater.* **2000**, *12*, 1122–1125.
- (25) Burger, A.; Wilson, E. L.; Brindley, C. O.; Bernheim, F. *J. Am. Chem. Soc.* **1945**, *67*, 1416–1419.
- (26) Li, H.; Powell, D. R.; Hayashi, R. K.; West, R. *Macromolecules* **1998**, *31*, 52–58.
- (27) Heck, R. F. *Palladium Regents in Organic Synthesis*; Academic Press: New York, 1990.
- (28) Hu, B.; Karasz, F. E. *Chem. Phys.* **1998**, *227*, 263–270.

MA020893A